

Preparation and Characterization of Zinc Oxide Nanoparticles for Use in Heterojunctions For Diodes and Solar Cells

Tyler Revie, Advisor: James Masi Ph.D

Department of Engineering

University of Southern Maine

Conductive and dielectric oxide-based nanoparticles have become a centerpiece for research in the scientific community over recent years. This work was conducted with the intent of developing a nano-particulate Zinc oxide chemistry which was easy to implement with low temperature fabrications methods and metastability considerations. A metal chloride approach was used resulting in the eventual oxidation of combinational variations of the oxides. The initial tests were made by measuring the size, shape, density, and distribution of the nanoparticles in suspension as well as the fluorescence and absorbance spectrums of ZnO and aluminum doped variant nanoparticles. The simplicity of the methods make possible application in both secondary and university labs.

Corresponding Author: Tyler M. Revie | Tyler.Revie@maine.edu

Introduction

Nanostructured wide-bandgap semiconductor (NWS) devices are made from group III nitride nanoparticles, including ZnO via variations of traditional semiconductor machining processes. The biggest difference is the deposition of group III nanoparticles on the surface of the semiconductor SI wafer in place of traditional group V dopants such as boron or phosphorus. Research suggests that the behaviors of nanostructured wide-bandgap semiconductor devices are similar to traditional semiconductor devices with few key differences creating niche use purposes. Differences include a higher band gap between the semiconductor's band gap, or electron energy required to excite an electron between the structure's valence and conduction bands, a greater specific heat capacity allowing for the structure to operate under higher thermal stresses for longer periods of time before going into a failure state, higher efficiencies, faster switching speeds, as well as the ability to handle higher voltages, powers, and frequencies. Additionally, wide bandgap devices may be implemented on a smaller scale while still being stable due to these properties.

These properties are partially determined by the material structure of the group III nanoparticle used to dope the semiconductor's SI layer and

partially determined by the size, shape, purity, and concentration of the nanoparticles used and therefore the conditions and methodologies used to create them. As such, it is of utmost importance to properly characterize and perform early stage product quality control to determine the physical size, shape, and number of nanoparticles present as well as their fluorescent and absorptive properties through traditional spectrophotometry.

To ensure proper test results and laboratory safety all steps performed within the nanoparticle synthesis phase as well as the material testing phase were done in accordance with all safety standards set forth by the University of Maine System, OSHA, and Fisher Scientific - the materials supplier for this project - regarding the handling of nanoparticles, general laboratory etiquette and safety, and chemical processes. Additionally, standards set by the National Nanotechnology Initiative in collaboration with the United States Food and Drug Administration, ASTM International, and the International Organization for Standardization (ISO). These standards include ASTM E2909-13 which is a standard guide for how reports regarding nanotechnologies should be written and reported, ISO 80004-1:2010, ASTM E2490-09(2015), ISO 13014:2012 and ISO 12901-1:2012 which outline nanotechnology nomenclature including prefixes, a general use guide

to measuring particle size in suspension by photon correlation spectroscopy (PCS), guidance on physio-chemical characterization of engineered nanoscale materials for toxicologic assessment, standard test method for hemolytic properties of nanoparticles, management of occupational risk and lab work associated to engineered nanomaterials, and a guide to education regarding nanotechnology health risks and how to best mitigate them. These cumulative safety and measurement standards were used to ensure the safety of lab personnel as well as preserve the purity of synthesized nanoparticles and required components.

Methodology

Experimental Setup

The synthesis process of zinc oxide and aluminum doped zinc oxide nanoparticles is a fairly simple one and does not require any special equipment or high temperatures. The procedure takes place at or near room temperature with the maximum required heat at any phase being 80°C (Jacobs). Zinc oxide nanoparticles are known for being synthesized using mostly mild materials, nevertheless chemical components are known irritants and toxic if ingested or otherwise inhaled in large enough quantities (). As such, material synthesis should be conducted in a fume hood inside a well-ventilated room while wearing proper PPE including but not limited to, gloves, safety glasses, and long clothing. As materials used to synthesize the nanoparticles as well as the resulting nanoparticle solutions are sensitive to impurities, clothing worn should be clean. A lab coat may be worn on site to limit potential contamination ()�.

The list of necessary lab equipment to perform satisfactory nanoparticle analysis follows: liquid particle analyzer, microscope, spectrophotometer capable of performing fluorescence and absorbance testing, particle counter (). The list of necessary reactants their respective quantities follows and materials required to prepare the nanoparticle solutions follow: 167mL Isopropyl Alcohol (C_3H_8O), 10 mL Ammonia (NH_3), 50 mL DI Water (H_2O) 26 mg Zinc Acetate Dihydrate ($C_4H_{12}O_6Zn$), 60 mg Aluminum Nitrate Nonahydrate ($Al(NO_3)_3 \cdot 9H_2O$), 35

mg Sodium Hydroxide (NaOH), Variable Quantity Citric Acid ($C_6H_8O_7$), glassware, beakers, hot plate, magnetic stirrer and stir bars, balance, spoons, pasteur pipettes, thermometers, fume hood.

Procedure: ZnO

To begin synthesizing zinc oxide nanoparticles, prepare two water baths by filling a large container capable of containing three beakers with water. Chill one water bath to 5°C and heat the other to 65°C. Place thermometers in water baths to monitor temperature over time. While the water baths are being brought to temperature, measure 17ml isopropyl alcohol and place in a beaker. Label the beaker “Sodium Hydroxide”. Then, measure 25ml isopropyl alcohol and place in a different beaker. Label this beaker “Zinc Acetate”.

Next, measure 125ml isopropyl alcohol and place it in a third beaker. Label it “Isopropyl”. Measure 35mg sodium hydroxide and introduce it to the “Sodium Hydroxide” beaker. Place “Sodium Hydroxide” beaker in fume hood on a hot plate with a magnetic stirrer. Deposit magnetic stir bar into beaker and stir the contents slowly while at low heat until the sodium hydroxide solute has entirely dissolved into the isopropyl solvent. While continuing to monitor the states of other components, measure 10g zinc acetate dihydrate and introduce it to the “Zinc Acetate” beaker. Place “zinc acetate” beaker in fume hood on a hot plate with a magnetic stirrer. Deposit magnetic stir bar into beaker and stir the contents slowly while on low heat until the zinc acetate dihydrate solute has entirely dissolved into the isopropyl solvent. Continue monitoring states of water baths and solutions until their respective processes have concluded.

When a solution has finished mixing, remove from the magnetic stirrer and hotplate but keep under the fume hood for safety. Once all processes have concluded, chill the contents of the “Sodium Hydroxide” beaker with the cold water bath. Do not mix the contents of the “sodium hydroxide” beaker and the cold water bath. Similarly, chill the contents of the “isopropyl” beaker with the cold water bath. Do not mix the contents of the “isopropyl” beaker and the cold water bath. Once all solutions have been

formed and required components chilled begin the final reaction by mixing the contents of the “Sodium hydroxide” beaker and “isopropyl beaker” on low heat within a fume hood. Introduce magnetic stir bars and stir vigorously. Once solution has begun rapidly stirring introduces the contents of the “Zinc Acetate” beaker.

Finally, use the hot water bath to shock the contents of the final beaker. Transport solution from beaker to sealable bottle and label its contents “ZnO”. The produced solution may be centrifuged for same-day settling and analysis. Clean used components as needed and prepare lab space for synthesis of aluminum doped variants.

Procedure: Al-ZnO

To begin synthesizing aluminum doped zinc oxide nanoparticles, fill a beaker with 50mL distilled water. Begin heating the beaker to 80°C. Place thermometers in the beaker to monitor temperature over time. While the beaker is warming, measure 16mg zinc acetate dihydrate and 60mg aluminum nitrate nonahydrate. Keep measured materials separated until the beaker is fully heated. Once the zinc acetate dihydrate and aluminum nitrate nonahydrate have been measured, fill a graduated cylinder with 10ml ammonia and have pure citric acid ready to be introduced to the solution as needed via pasteur pipette or similar device.

Once the distilled water has been heated, remove the thermometer from the beaker and place it under a fume hood on top of a magnetic stirrer. Place a magnetic stir bar within the heated water and set the strength to high. Next, introduce the 16g of zinc acetate dihydrate to the water. Then, introduce the 60mg aluminum nitrate nonahydrate to the water. Immediately begin adding citric acid to the solution, checking the pH level between additions. Continue adding citric acid until the pH of the solution measures 1.5.

If at any time too much citric acid has been introduced, add more water to the device solution and add heat. Once the pH has settled at 1.5, add the 10mL of ammonia to the solution. Allow the solution to stir for sixty seconds after the addition of the ammonia. After the sixty seconds have elapsed, turn

off the heat source, magnetic stirrer, and remove contents from the fume hood. Transport solution from beaker to sealable container and label its contents “Al:ZnO”. The produced solution may be centrifuged for fast same-day settling and analysis. Clean used

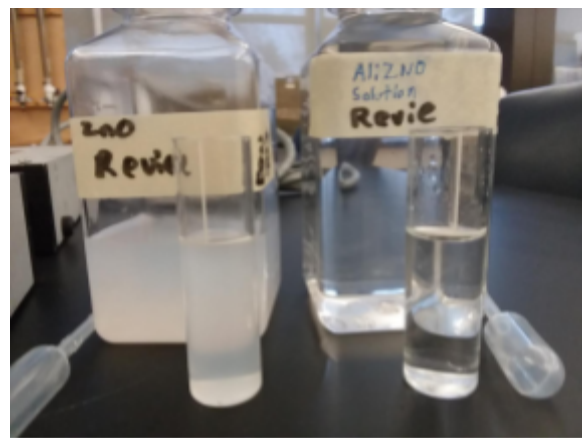


Figure 1: ZnO & Al:ZnO Nanoparticles in Suspension

components and lab space as needed. Prepare for material analysis and testing.

Initial Results & Imaging

Visual inspection of prepared ZnO and Al:ZnO nanoparticle solutions conducted with no imaging devices or aids are non-conclusive. Produced solutions were determined to consist of nanoparticles too small to be seen by the blind eye, in too small a concentration to be visible within the solutions, or otherwise not present within the samples. Figure 1.



Figure 2: uLPS System

shows the nanoparticle solutions following synthesis on the macro scale. The solution on the left are the ZnO nanoparticles suspended in isopropyl alcohol

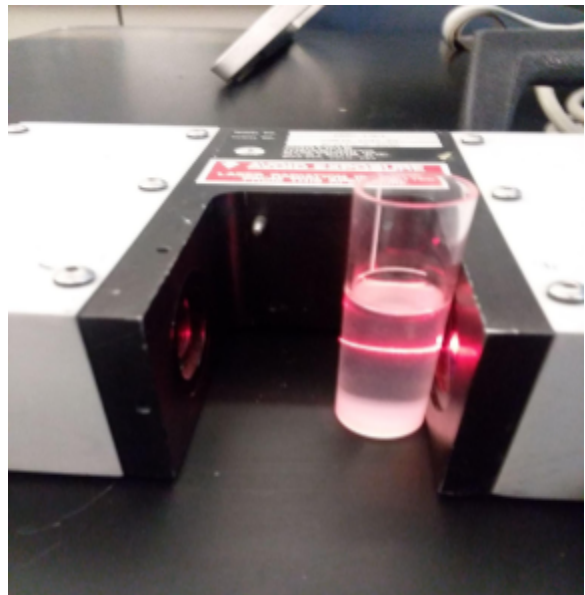


Figure 3: 15mL Al:ZnO Solution Measured by uLPS Laser

while the solution on the right are the Al:ZnO nanoparticles suspended in DI water.

It can be seen that no nanoparticles are visible either within the larger containers nor the 15ml samples. In order to determine if nanoparticles are present, Particle Measuring Systems Inc. Micro Laser



Figure 4: Sebago Scientific AIM-10

Particle Spectrometer uLPS device was used to verify the presence of particulates in the solutions and determine their size, if proven present. Figure 2, shows the system used to measure the preliminary particle size while Figure 3 shows a 15ml sample of Al:ZnO being tested by the uLPS's laser apparatus. uLPS testing suggested that thousands of

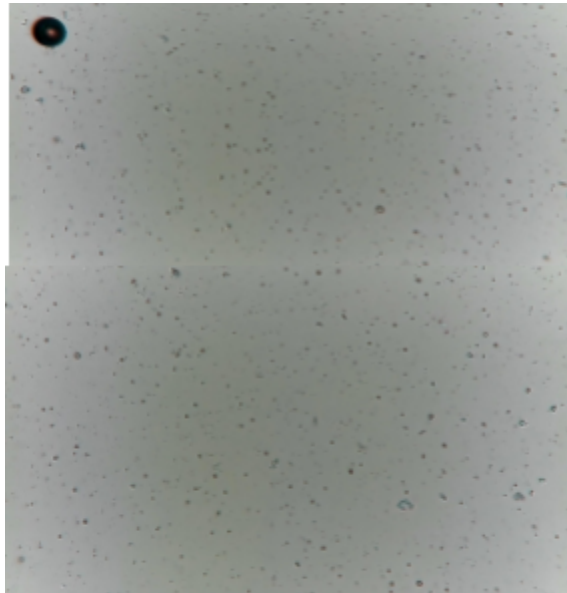


Figure 5: ZnO Nanoparticles at 100x Magnification

nanoparticles were present per 15ml sample within both ZnO and Al:ZnO solutions and that the majority of samples were under 300 nanometers in volume.

As the uLPS system is incapable of performing imaging or more precise measurement the samples were moved to the imaging lab where they were tested, counted, and imaged using a Sebago Scientific AIM-10 Liquid Particle Analyzer as shown in Figure 4. To operate the Sebago Scientific device, sample solutions of both ZnO and Al:ZnO were taken and individually inserted into the AIM-10's liquid tray. On the accompanying computer apparatus "start test" was selected and after several minutes the tests were automatically completed and data regarding the nanoparticle's size, shape, distribution, and other physical qualities were readily available alongside 50 photographs taken of each sample at 100x magnification.

Operation of the AIM-10 device as well as photos and datasets generated proved that

nano particles were present in the samples as well as a general idea of what they looked like at significant enough of a magnification factor to make them visible. Figure 5 shows two photos of the ZnO nanoparticles taken by the AIM-10 while Figure 6

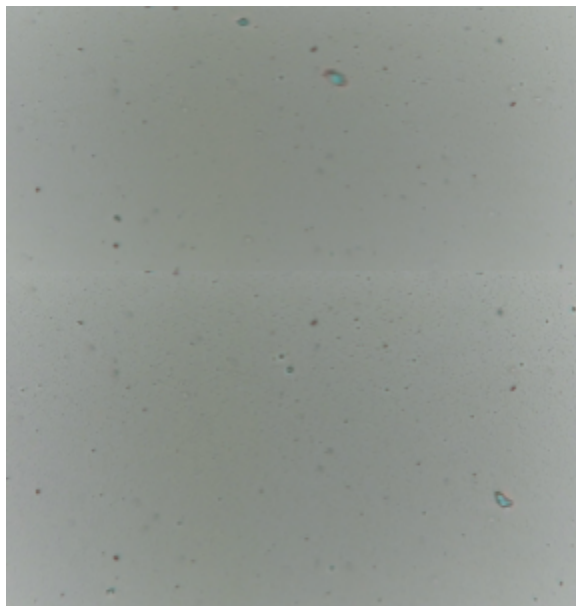


Figure 6: Al:ZnO Nanoparticles at 100x Magnification

shows two photos of the Al:ZnO nanoparticles taken by the AIM-10.

Inspection of photos suggests that the Al:ZnO particles are smaller than the ZnO particles, have greater size uniformity than the ZnO particles, have more distance between them in the solution than the ZnO particles, are less spherical than the ZnO particles, and are less numerous than the ZnO particles. In order to verify these observations the data gathered by the AIM-10 device during both ZnO and Al:ZnO testing was exported as a .csv file and further analyzed with excel and graphical methods.

Test Results

Tabulated data exported from the AIM-10 device for both ZnO and Al:ZnO testing can be seen in Table

| Measurement | Mean | Median | Std Dev | Min | Max | % CV | Range | Variance | Mode | Skewness | Greenian |
|-------------|----------|--------|----------|----------|-------|---------|----------|----------|--------|----------|----------|
| ESD | 3.82 | 2.49 | 10.02 | 517.3 | 5.77 | 262.3 | 511.52 | 300.5 | 5.8 | 38.51 | 3.19 |
| ABD | 2.82 | 2.34 | 3.75 | 179.28 | 0 | 140.07 | 178.28 | 23.58 | 1.05 | 38.84 | 0 |
| Perimeter | 12 | 9.08 | 10.48 | 1624.01 | 5.96 | 262.08 | 1618.75 | 996.9 | 5.97 | 38.51 | 10 |
| Width | 21.18 | 9 | 31.4 | 2528 | 1 | 280.06 | 2523 | 986.25 | 7 | 42.44 | 9.52 |
| Height | 9.93 | 8 | 23.31 | 3088 | 5 | 216.62 | 3079 | 462.69 | 6 | 48.85 | 8.5 |
| Area | 18.48 | 4.29 | 408.27 | 25228.42 | 0 | 2317.48 | 25228.42 | 180481.7 | 2.14 | 44.36 | 0 |
| Focus | 485.05 | 385.38 | 5480.12 | 5.99 | 85.48 | 5480.12 | 53801.7 | 5.49 | 2.6 | 382.61 | 0 |
| AverageR9 | 189.88 | 206.42 | 23.81 | 325.03 | 48.45 | 214.49 | 181.38 | 557.37 | 87.29 | 1.39 | 187.59 |
| AverageR9 | 314.8 | 310.42 | 22.03 | 331.21 | 49.4 | 29.17 | 181.81 | 484.24 | 96.11 | 1.43 | 132.99 |
| AverageR11 | 115.27 | 111.38 | 21 | 242.8 | 48.82 | 18.22 | 120.58 | 440.89 | 300.33 | 1.4 | 113.57 |
| AspectRat | 1.21 | 1.08 | 0.58 | 13 | 0.67 | 47.99 | 31.99 | 0.33 | 1 | 3.76 | 1.12 |
| Transpare | 59.15 | 58.09 | 3.95 | 85.72 | 4.9 | 20.08 | 75.82 | 25.45 | 4.9 | 1.59 | 50.87 |
| Intensity | 44.46 | 42.87 | 8.76 | 89.17 | 19.8 | 29.98 | 69.93 | 76.35 | 37.72 | 1.37 | 41.7 |
| Circularity | 0.95 | 0.72 | 0.19 | 0.94 | 0 | 29.23 | 0.94 | 0.04 | 0.03 | -0.96 | 0 |
| CPVs | 25487.06 | 12.59 | 3029152 | 70440556 | 2.95 | 4794.06 | 70440548 | 1.09E+12 | 3.60 | 55 | 36.93 |
| CPVs | 1070.31 | 6.68 | 44469.52 | 3614793 | 0 | 4143.21 | 3614793 | 1.98E+09 | 2.38 | 48.87 | 0 |

Table 1: Physical Properties of ZnO Nanoparticles

1 and Table 2 respectively. Material size and shape data points are measured in nanometers while transparency and intensity values are represented as percentages. Circularity data is on a scale of 0-1 with higher values representing more circular particles.

Data show that ZnO particles have a smaller mean and median than the Al:ZnO particles and are more uniformly shaped across ESD and ABD measurements. Data show that ZnO particles are more circular than the Al:ZnO particles and that the Al:ZnO particles are more transparent than the prepared ZnO particles.

| Measurement | Mean | Median | Std Dev | Min | Max | % CV | Range | Variance | Mode | Skewness | Greenian |
|-------------|----------|--------|----------|----------|-------|--------|----------|----------|---------|----------|----------|
| ESD | 14.14 | 3.12 | 58.58 | 595.26 | 1.78 | 414.25 | 528.5 | 3431.44 | 1.88 | 8.62 | 4.96 |
| ABD | 4.7 | 1.62 | 14.72 | 137.32 | 0.28 | 113.19 | 137.86 | 266.79 | 0.94 | 6.28 | 1.92 |
| Perimeter | 44.39 | 9.74 | 105.94 | 1085.02 | 5.34 | 414.37 | 1025.48 | 33032.09 | 5.03 | 8.62 | 12.75 |
| Width | 50.25 | 12 | 208.52 | 1520 | 1 | 458.75 | 1567 | 52138.36 | 9 | 7.27 | 14.21 |
| Height | 24.08 | 3.9 | 99.4 | 1090 | 3 | 275.98 | 3577 | 4485.03 | 8 | 7.85 | 12.22 |
| Area | 187.53 | 2.06 | 1221.61 | 14862.16 | 0.06 | 651.42 | 14862.1 | 14862.1 | 14862.1 | 7.66 | 2.9 |
| Peris | 96.76 | 46.58 | 117.57 | 1044.85 | 3.73 | 123.52 | 2855.12 | 2855.12 | 2855.12 | 28.68 | 3.79 |
| AverageR9 | 131.11 | 136.32 | 28.89 | 289.45 | 46.36 | 15.72 | 161.89 | 437.96 | 130.93 | -0.44 | 131.32 |
| AverageR9 | 138.7 | 142.89 | 28.29 | 223.09 | 38.3 | 14.39 | 182.39 | 403.96 | 129.98 | -0.8 | 137.1 |
| AverageR11 | 134.67 | 137.23 | 19.27 | 212.17 | 45.88 | 14.38 | 166.34 | 375.03 | 138.33 | -0.64 | 132.12 |
| AspectRat | 1.33 | 1.12 | 0.89 | 35.99 | 0.23 | 69.91 | 38.25 | 0.72 | 1 | 3.79 | 1.17 |
| Transpare | 93.14 | 70.29 | 8.21 | 89.87 | 65.51 | 67.45 | 24.08 | 87.45 | 46.09 | -0.37 | 68.43 |
| Intensity | 55.56 | 59.02 | 7.9 | 85.1 | 25.39 | 14.75 | 65.75 | 82.44 | 43.82 | -0.52 | 52.95 |
| Circularity | 0.31 | 0.22 | 0.23 | 0.32 | 0.02 | 76.39 | 0.89 | 0.05 | 0.08 | 0.8 | 0.22 |
| CPVs | 773778.2 | 13.69 | 3048978 | 70527504 | 2.87 | 758.84 | 70527503 | 3.42E+15 | 3.35 | 8.59 | 35.81 |
| CPVs | 12146.91 | 2.23 | 96717.68 | 1255089 | 0.02 | 746.88 | 1255089 | 1.26E+09 | 0.43 | 8.36 | 3.71 |

Table 2: Physical Properties of Al:ZnO Nanoparticles

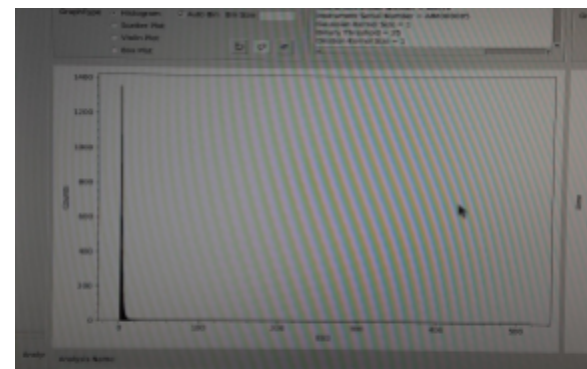


Figure 7: Particle Size Analysis of ZnO

To accurately measure the number of particles present, AIM-10 data was used to graph the ESD particle size in nm versus the number of counts of particles at that size. Figures 7 and 8 show the 3D size of the nanoparticles measured in ESD nanometers on the x axis as well as the number of particles of that given size counted on the y axis.

Data show the ZnO solution has 1300 particles at its median size, 3.9 nanometers ESD. Similarly, data show Al:ZnO solution has 600 particles at its median

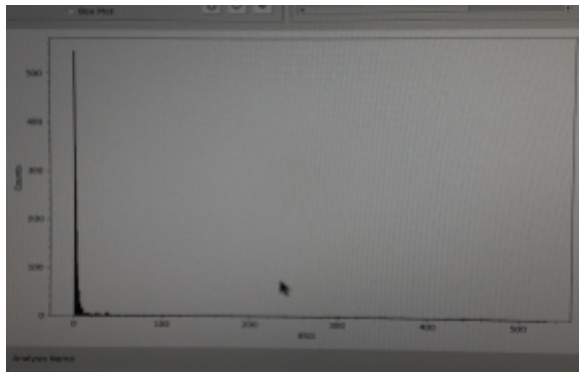


Figure 8: Al:ZnO Particle Size Analysis

size 3.1 nanometers ESD.

With the particles counted, sized, visually inspected, and otherwise analyzed according to their visual properties particle solutions underwent fluorescent and absorbance mode spectrophotometry analysis to test the material's bandgaps and properties in an attempt to estimate its behavior when used to create a semiconductor.

Fluorescence and absorption tests were conducted with a Vernier Spectrovis

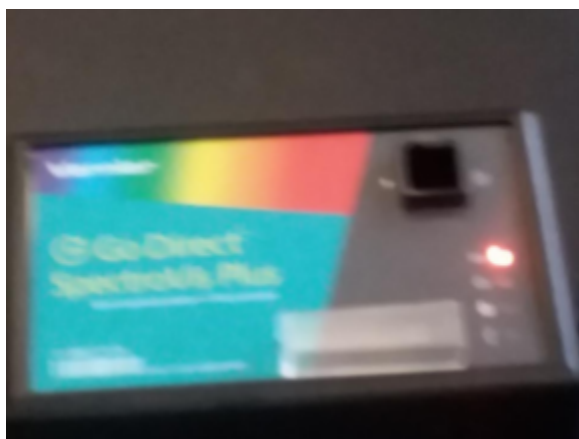


Figure 9: SpectroVis Spectrophotometer

spectrophotometer as shown in Figure 9.

Results of fluorescence mode testing of ZnO and Al:ZnO solutions are shown in Figures 10 and 11 respectively. Peak wavelength, known as the ROI (Region of Interest) of the fluorescence test shows which band gap the material used to emit photons when excited electronically or thermally. The data can then be used to determine the color and range of

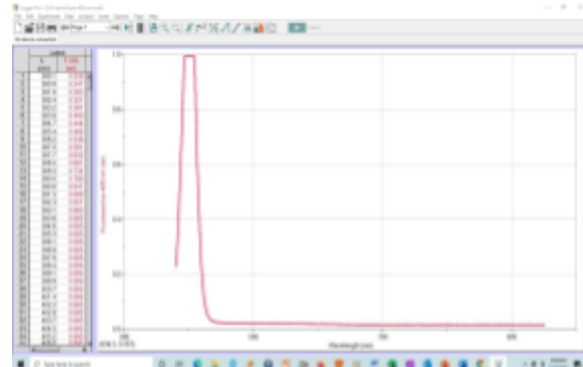


Figure 10: Fluorescence Test Results ZnO

these emissions.

Data show the fluorescence test results of both ZnO and Al:ZnO are similar. Peak ROI of ZnO solution was shown to correlate with a wavelength of 405nm, the violet region of the visible light spectrum. Despite 2% aluminum doping, Al:ZnO particles had a Peak ROI at approximately 410nm, still within the violet region of the visible light spectrum.

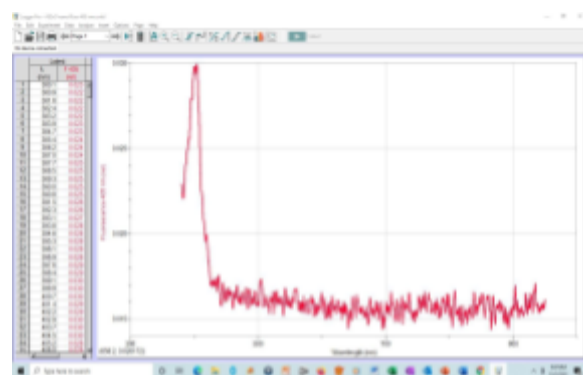


Figure 11: Fluorescence Test Results Al:ZnO

The test mode of the Vernier Spectrovis was switched and absorption testing was conducted using

the same methodology, but with different goals and analysis parameters. While fluorescence testing measures the output capability of the system, absorption testing measures its input capacity: what wavelengths of light it can be excited by, what color light does this wavelength correlate to, what is the energy gap of the material's band gap and what is the energy of the material's electron layers. Results of the absorbance tests of ZnO and Al:ZnO nanoparticles are shown in figures 12 and 13 respectively. Data show ZnO nanoparticles absorb violet, blue, and potentially green light with wavelengths between 400 and 550 nanometers. Data show Al:ZnO nanoparticles absorb violet and blue light with Wavelengths between 450 and 525 nanometers.

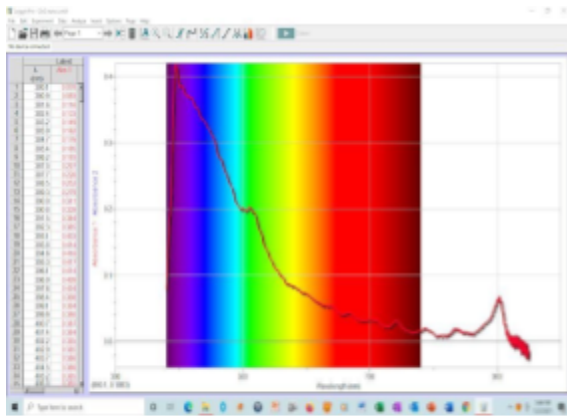


Figure 12: Absorbance Test Results ZnO

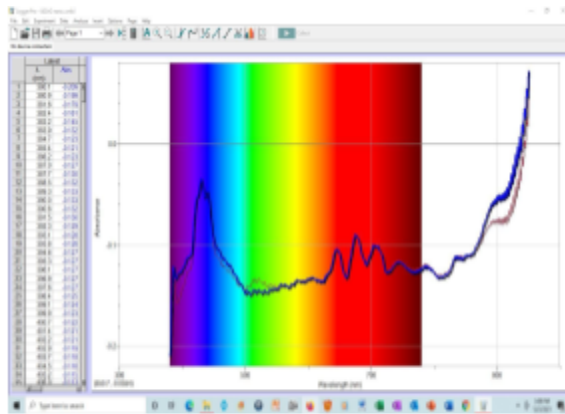


Figure 13: Absorbance Testing Results Al:ZnO

The wavelength associated with the material's peak absorbance can be used to calculate the energy

gap of the material's band gap in eVs and Joules by using the data in equation 1.

$$BeV = \frac{1240}{\lambda p} \quad (1)$$

Where λp is the wavelength associated with the peak absorbance value, and BeV is the energy gap of the band gap measured in electron volts. Equation (1) is a simplified form of the proper equation

$$BeV = \frac{h*c}{\lambda p} \quad (2)$$

Where λp is the wavelength associated with the peak absorbance value, BeV is the energy gap of the band gap measured in electron volts, h is the speed of light $3 * 10^8$ m/s, h is Planck's Constant, $6.6 * 10^{-34}$ J*s. The equivalent value in Joules may be calculated by multiplying the BeV value in electron volts by multiplying by $1.6 * 10^{-19}$ J.

A similar process may be used to determine the energy of one of the material's electron layers by taking the slope of the line immediately as peak absorbance begins to decrease and extrapolating data until it crosses the X axis. The frequency of this wavelength of light, known as λx may be used in place of λp in equations (1) and (2) to either estimate or calculate the energy of this layer. The capacities of these layers as well as the wavelengths of light used to calculate them, λp and λx are shown in Table 3.

| Material | λp (nm) | λx (nm) | BeV | EeV |
|----------|---------------------|---------------------|-------|------|
| ZnO | 405 | 580 | 3.06 | 1.09 |
| Al:ZnO | 450 | 525 | 2.755 | 2.43 |

Table 3: Absorbance Wavelength and Band Gaps of Materials

Analysis

Results suggest that the nanoparticles created have band gaps within the acceptable regions of the material's synthesized. The theoretical band gap of Zinc Oxide nanoparticles is thought to be between 3.0-4.0 eVs depending on particle size, shape, and

concentration during spectrophotometry analysis. Smaller nanoparticles are thought to produce higher bandgap materials, while more circular particles at higher concentrations are also thought to produce higher bandgap materials. While the ZnO nanoparticles synthesized in the lab are very small, with an average size of 3.92 nanometers ESD, many outliers do exist and the standard deviation is relatively high, suggesting these outliers are large but not plentiful in solution. These outliers, combined with the low circularity and relatively low particle count as well as the suspension agent itself all work to lower the eV value of the bandgap. Additionally, Al:ZnO doping produced very little difference in fluorescence testing results, but significantly reduced the absorbance of the material and the band gap of the material, going from 3.06 to 2.755eV and significantly increasing the EeV of the material, going from 1.09eV for Zinc Oxide to 2.43eV for Aluminum Doped Zinc oxide.. This is thought to be due to the conductive nature of aluminum and the low 2% doping percent.

Conclusion

The nanoparticles synthesized in the lab have properties within the acceptable theoretical and predicted ranges considering equipment limitations. As such, the project may be considered a success as nanoparticles were prepared and characterized for use in further study. Further studies will expand upon many of the tests and results conducted on the nanoparticles in suspension form and include performing conductivity testing on the powders once separated from solution, performing spray pyrolysis of the nanoparticles onto quartz thin films and measuring optical properties and conductivity, performing spray pyrolysis of the nanoparticles onto silicon crystals for heterojunction synthesis, and the formation of photovoltaics and UV detectors from the created heterojunction devices.

Acknowledgements

Authors acknowledge support and funding received from USM UROP (Undergraduate Research

Opportunities Program), its members and staff for making this project possible.

References

1. Authors, A., & Singh, M. (n.d.). Size and shape effects on the band gap of semiconductor compound nanomaterials. Retrieved from <https://www.tandfonline.com/doi/full/10.1080/16583655.2018.1473946>
2. Davis, K., Yarbrough, R., Froeschle, M., White, J., & Rathnayake, H. (2019, May 10). Band gap engineered zinc oxide nanostructures via a sol–gel synthesis of solvent driven shape-controlled crystal growth. Retrieved from https://pubs.rsc.org/en/content/article_landing/2019/ra/c9ra02091h
3. Davis, S. (2018, May 31). Power Management Chapter 11: Wide Bandgap Semiconductors. Retrieved from <https://www.powerelectronics.com/technologies/power-management/article/21864166/power-management-chapter-11-wide-bandgap-semiconductors>
4. Gupta, A., Srivastava, P., Bahadur, L., Amalnerkar, D., & Chauhan, R. (2014, November 28). Comparison of Physical and Electrochemical Properties of ZnO Prepared via Different Surfactant-Assisted Precipitation Routes.
5. Herrero, Y. R., & Ullah, A. (2020, June 05). Metal oxide powder technologies in catalysis. Retrieved from

<https://www.sciencedirect.com/science/article/pii/B9780128175057000142>

6. Jacobs, A., & Lisensky, G. (n.d.). Synthesis of Zinc Oxide Nanoparticles.

7. Liao, M., Stergiopoulos, T., Alvarez, J., Chattopadhyay, S., & Zhang, G. (2015, October 28). Wide-Bandgap Semiconductors: Nanostructures, Defects, and Applications. Retrieved from <https://www.hindawi.com/journals/jnm/2015/713896/>

8. McGlynn, E., Henry, M., & Mosnier, J. (2010, February 11). ZnO wide-bandgap semiconductor nanostructures: Growth, characterization and applications. Retrieved from <https://www.oxfordhandbooks.com/view/10.1093/oxfordhb/9780199533053.001.0001/oxfordhb-9780199533053-e-14>

9. P. (n.d.). Measuring Band Gap Energy of Doped Zinc Oxide Nanoparticles. Retrieved from https://www.perkinelmer.com.cn/CM_SResources/Images/46-74327APP_UVVISNIRMeasureBandGapEnergyValue.pdf

10. Sangiorgi, N., Aversa, L., Tatti, R., Verucchi, R., & Sanson, A. (2016, November 26). Spectrophotometric method for optical band gap and electronic transitions determination of semiconductor materials. Retrieved from <https://www.sciencedirect.com/science/article/abs/pii/S0925346716306395?via=ihub>

11. Shideh, A., Nilofar, A., Alghoul, M., Hammadi, F., Saeedfar, K., Ludin, N., . . . Sopian, K. (2014, February 09). The Role of Physical Techniques on the Preparation of Photoanodes for Dye Sensitized Solar Cells.

12. Standards for Nanotechnology. (n.d.). Retrieved from <https://www.nano.gov/you/standards>

13. Timothy, H., & Masi, J. (n.d.). Preparation and Properties of Nano-Particulate Conductive and Dielectric Oxides via Co-Precipitation Using Various Chloride Sources.

14. Waegeneers, N., DeVos, S., Verleysen, E., Ruttens, A., & Mast, J. (2019, August 22). Estimation of the Uncertainties Related to the Measurement of the Size and Quantities of Individual Zinc Oxide Nanoparticles. Retrieved from <https://www.ncbi.nlm.nih.gov/pmc/articles/PMC6747558/>

15. What are Nanoparticles? Definition, Size, Uses and Properties. (n.d.). Retrieved from <https://www.twi-global.com/technical-knowledge/faqs/what-are-nanoparticles>

